

Calculation of Hydrogen Buildup in the Neighborhood of Intergranular Cracks

T. I. Zohdi¹ and E. I Meletis²

Abstract

Based on previous experimental observations and theoretical predictions, it has been proposed that the intergranular hydrogen embrittlement process involves the nucleation of an incremental crack at the edge of the plastic zone that extends backwards and joins the original macrocrack but also forwards in the region that is stressed above a critical stress level and has relatively high hydrogen concentration. These predictions of the crack jump distance are in excellent agreement with the experimental observations[2]. The velocity of the individual intergranular crack jumps was estimated to be about one and a half orders of magnitude higher than the experimentally observed overall crack velocity, suggesting that fracture of ligaments separating parallel but displaced intergranular cracks is the controlling process. Numerical experiments conducted in the present work, retaining an often neglected reaction term, show that the hydrogen diffusion rates are grossly underestimated if the reaction term is discarded. Furthermore, numerical experiments corroborate the hypothesis in [2] that fracture of the ligament is initiated at the plastic-elastic interface and the macrocrack itself is the rate controlling step in the hydrogen embrittlement fracture process.

1 INTRODUCTION

One of the most common causes of failure in engineering structures is related to the presence of hydrogen which can cause embrittlement in a variety of materials ranging from conventional materials to advanced alloys, intermetallics and ceramics. Hydrogen frequently comes into contact with engineering structures as product of corrosion, electroplating or other processes. Hydrogen is introduced in materials in atomic form (H) either electrolytically or from a gaseous atmosphere. Hydrogen embrittlement (HE) is a mechanical-environmental failure that results from the initial presence or absorption of hydrogen in metals, usually in combination with residual or applied tensile stresses. Hydrogen embrittlement results in subcritical crack growth at loading levels significantly lower than those associated with unstable (hydrogen free) crack motion. Cracking caused by this process is often referred to as hydrogen-stress cracking and hydrogen-induced cracking. It has been suggested that hydrogen enhances cracking because hydrogen absorption at these sites lowers the surface energy required for cracks to grow; hydrogen reduces the bonding energy of the metal lattice

¹ Institut für Mechanik, D-64289 Darmstadt, Germany

²Department of Mechanical Engineering, Louisiana State University

sufficiently to allow cracking and hydrogen enhances localized plastic deformation. In any event, hydrogen diffusion seems to be an important element in most HE mechanisms [1].

In this paper, we propose the notion that after a microcrack has initiated at the plastic/elastic interface, which requires a relatively short period of time [2], the bonds in the zone between the microcrack and macrocrack have to be sufficiently weakened for the microcrack to extend backwards to join the macrocrack. This occurs when sufficient hydrogen diffuses in front of the crack tip, and the average concentration in the plastic zone exceeds some critical value (depending on the material and some appropriate stress threshold [3]) then the microcrack can join the macrocrack by propagating backwards through the sufficiently weakened material. If the initiation is in the vicinity of the original crack, then this microcrack will grow until it rejoins the macrocrack, leading to the appearance of macrocrack "growth" or "propagation".

A simple constitutive model relating the flux of a small solute diffusing in a stressed solid is given by modified form of Fick's law incorporating pressure gradients into the diffusion equation [4]

$$\mathcal{F} = -\{\mathcal{D}\nabla c + \mathcal{D}\epsilon c\nabla\mathcal{P}\} \quad (1)$$

where c is the concentration of the solute, \mathcal{P} is the *hydrostatic pressure* ($= -tr\sigma/3$, σ being the stress present in the body), ϵ and \mathcal{D} are positive constants, where $\epsilon \approx \mathcal{O}(10^{-5})(Pa)^{-1}$. The parameter ϵ typically depends on the temperature, the universal gas constant and the partial molar volume of the diffusing species. Upon substituting this relation into the conservation law, $\dot{c} + \nabla \cdot \mathcal{F} = 0$, one obtains the following equation governing the diffusion of a dilute solute in a stressed solid

$$\dot{c} = \underbrace{\mathcal{D}\nabla^2 c}_{\text{Diffusion}} + \underbrace{\mathcal{D}\epsilon\nabla c \cdot \nabla\mathcal{P}}_{\text{Convection}} + \underbrace{\mathcal{D}\epsilon c\nabla^2\mathcal{P}}_{\text{Reaction}}. \quad (2)$$

Observe that this equation is parabolic, as is the classical diffusion equation. In the present work this is termed the *Diffusion-Convection-Reaction Model, DCR*. It can be noted that if the hydrostatic pressure field is harmonic the last term vanishes. For a detailed derivation of this equation, see [5], [6], [7]. Essentially, the idea is that for sufficiently small deformations the diffusion is affected by the change in volume of the microstructure (i.e. by the hydrostatic component of stress).

In many studies, the reaction term is neglected, even in elasto-plastic regimes, (see [1], [2], [3], [6]) which yields

$$\dot{c} = \underbrace{\mathcal{D}\nabla^2 c}_{\text{Diffusion}} + \underbrace{\mathcal{D}\epsilon\nabla c \cdot \nabla\mathcal{P}}_{\text{Convection}}. \quad (3)$$

This will be termed the *Diffusion-Convection Model (DC)*.

The ad hoc application of equations (2) and (3) has appeared repeatedly in materials science literature. *The use of the diffusion-convection equation can only be justified when the hydrostatic stress is harmonic.* This is not in general true for plastic stresses, and elastic stresses in the presence of a temperature field and/or body forces. Although in some cases, even if the stress field is not harmonic, one could justify the neglection of the reaction term

for an appropriate time scale or some other justifiable but *approximate* reason. For instance, one might argue that for short time scales encountered in applications that the reaction term does not have enough time to affect the solution. *The purpose of the present work is to demonstrate that, in the presence of environmentally-induced sharp cracks, the neglection of the reaction term in elasto-plastic fracture mechanics leads to gross underestimation of hydrogen buildup in the plastic zone, regardless of the time scale involved. In other words, the reaction term contributes almost instantly.*

2 THE MODEL PROBLEM

We consider a model problem of an intergranular crack with hydrogen atoms adsorbed at the root with remote uniaxial loading causing the stress field in the solid. This is shown in Figure 1. The source of H can be either a gas or liquid with the resulting hydrogen atoms adsorbed into the metal. Thereafter they diffuse into the metal structure towards the region of highest hydrostatic pressure. The mathematical idealization is the diffusion of hydrogen ahead of an intergranular crack into an elasto-plastic solid, as shown in Figure 2.

One dimensional models (along the $\theta = 0$ axis) of the two regimes DC and DCR will be used. This is justified from the fact that in the present case grain boundaries are aligned perpendicular to the stress axis. Thus, in these intergranular cases the diffusion rate is significantly faster ($\approx 10^3$ times greater) along these paths and essentially the flow is one dimensional. The coefficients of reaction and convection terms are quite large due to the fact that they are inversely proportional to the size of the crack tip radius. Particularly critical is the reaction term which is several orders of magnitude larger than either the diffusion term or convection term, owing to its dependence of the inverse of the square of the crack tip radius.

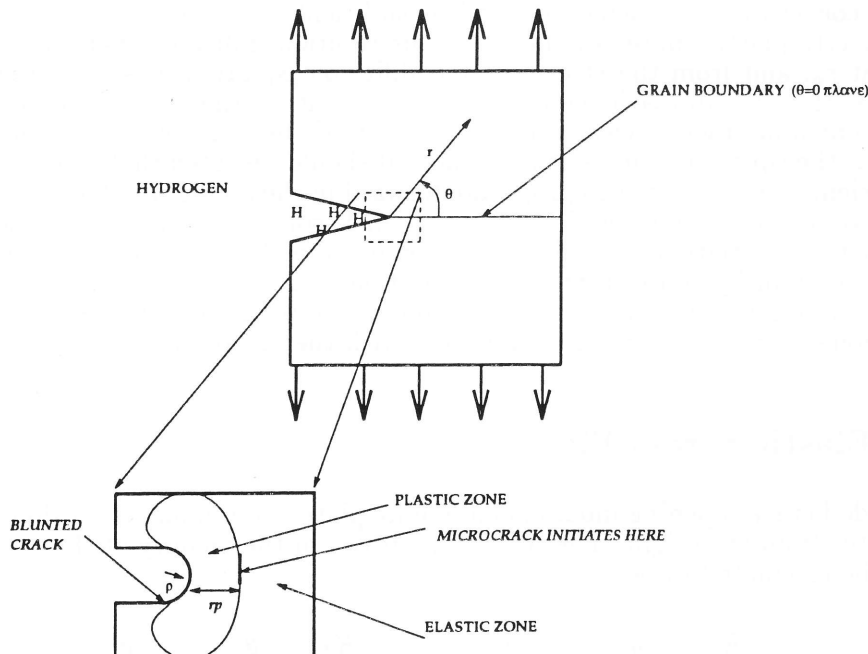


Figure 1: The model problem

For plane strain and assuming a perfectly elastic-plastic solid with no work hardening, Hill's slip line field equation for the hydrostatic pressure in the plastic zone is used immediately ahead of a blunted crack of radius ρ given by [8]

$$\mathcal{P} = -\sigma_{yield} \left[\ln \left(1 + \frac{r}{\rho} \right) + \frac{1}{2} \right] \quad (4)$$

where σ_{yield} is the material's yield strength, r is the distance ahead of the crack tip and \mathcal{P} is the hydrostatic pressure in the plastic zone. Note that this function is not harmonic. A frequently used relation for crack tip radius [3] is

$$\rho = \frac{K_I^2}{2\sigma_{yield}E} \quad (5)$$

and for the plastic zone size ([2]), r_p^*

$$r_p^* = (1 - 2\nu)^2 \frac{K_I^2}{2\pi\sigma_{yield}^2} \quad (6)$$

where K_I is the mode-I stress intensity factor, ν is the Poisson ratio, and E is the elastic modulus. Stress and strain distributions in the plastic zone, measured as well as calculated, can be found in [9], and are in qualitative agreement with the results of the classical treatment by Hill for plane strain assuming an elastic-perfectly plastic solid with no work hardening[10].

It is reasonable to assume that the crack will advance when a critical combination of stress and hydrogen concentration is achieved which is sufficient to produce cracking. Assuming an elastic-perfectly plastic material, the stress distribution indicates that the stress level is maximum at r_p , and from the stress-assisted diffusion equation it is expected that the hydrogen concentration will reach the critical level first at r_p , the edge of the plastic zone. Thus, the incremental crack nucleates in the vicinity of the edge of the plastic zone and extends towards the tip of the original macrocrack. It should be noted that if the incremental crack has sufficient energy it can also propagate forward in the region which is stressed above a critical hydrostatic pressure level (\mathcal{P}_c) and has high H concentration. Furthermore, it can be assumed that the initiation of a microcrack comes from the violation of a critical stress level similar to that in [3] coupled with an absorption of a critical amount of hydrogen in the plasticized material. This allows for weakening of the bonds and brittle fracture of the entire plastic zone allowing the microcrack to join with the macrocrack.

2.1 The Elastic Stress Field

Consider a mode I crack (opening mode) in an infinite plate under uniaxial tension and using polar coordinates from the origin. The principal stresses in the vicinity of the crack tip (see Figure 1) can be calculated to be

$$\sigma_1 = \frac{K_I}{\sqrt{2\pi r}} \cos \frac{\theta}{2} \left(1 + \sin \frac{\theta}{2} \right) \quad \sigma_2 = \frac{K_I}{\sqrt{2\pi r}} \cos \frac{\theta}{2} \left(1 - \sin \frac{\theta}{2} \right) \quad (7)$$

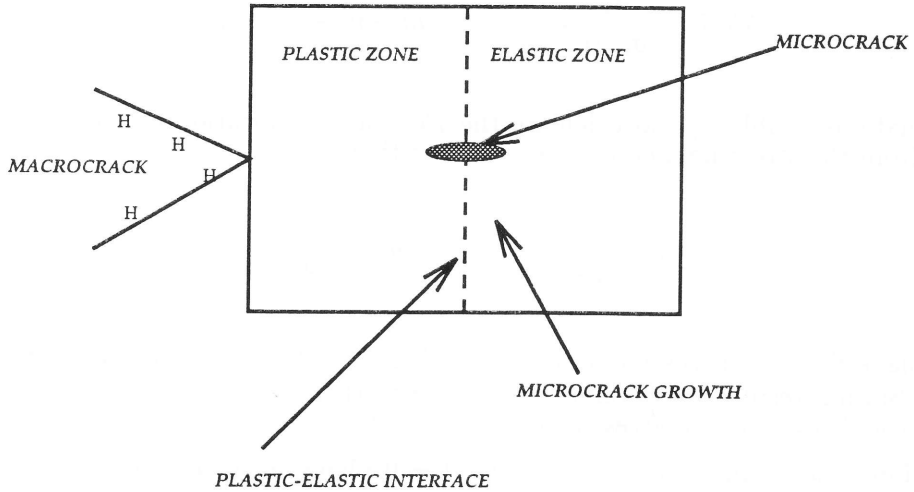


Figure 2: Proposed regime for the growth of the microcrack

For plane-strain regimes the third stress component is

$$\sigma_3 = \nu(\sigma_1 + \sigma_2) = 2\nu \frac{K_I}{\sqrt{2\pi r}} \cos \frac{\theta}{2}. \quad (8)$$

and for plane-stress regimes $\sigma_3 = 0$. The elasticity solution gives singular values for the stress at the crack tip, which is unrealistic. There is clearly a plasticized region in front of the crack, *the process-zone*. Typically in the vicinity of the process-zone the stress field will be a hybrid of both plane-strain and plane-stress states of stress. The hydrostatic pressure for both cases is given by

$$\mathcal{P} = -\left\{ \frac{2(1+\nu)}{3} \frac{K_I}{\sqrt{2\pi r}} \cos \frac{\theta}{2} (1 + \sin \frac{\theta}{2}) \right\} \quad \text{plane-strain}$$

$$\mathcal{P} = -\left\{ \frac{2}{3} \frac{K_I}{\sqrt{2\pi r}} \cos \frac{\theta}{2} (1 + \sin \frac{\theta}{2}) \right\} \quad \text{plane-stress}$$

$$\nabla^2 \mathcal{P} = 0$$

The plane strain plastic zone is significantly smaller than the plane stress plastic zone. This is a result of the fact that the effective yield stress in plane strain is larger than the uniaxial yield stress. The maximum stress in the plane strain plastic zone can be as high as three times the uniaxial yield stress. Using common terminology, we denote the ratio of the maximum stress to the yield stress, as the *plastic constraint factor*, $\mathcal{PCF} \stackrel{\text{def}}{=} \frac{\sigma_{\max}}{\sigma_{yield}}$. The quantity $\mathcal{PCF} \times \sigma_{yield}$ can be considered as an effective yield stress. The \mathcal{PCF} for the plane strain crack problem can be estimated in a standard straightforward manner. Taking $\sigma_2 = n\sigma_1$ and $\sigma_3 = m\sigma_1$, and using the Von Mises yield criterion, it is easy to show that

$$\mathcal{PCF} = \frac{\sigma_1}{\sigma_{yield}} = (1 - n - m + n^2 + m^2 - mn)^{-\frac{1}{2}} \quad (10)$$

These equations enable one to calculate the \mathcal{PCF} at any location of the crack tip region. Directly from the stress field equations it follows that

$$n = \frac{1 - \sin \frac{\theta}{2}}{1 + \sin \frac{\theta}{2}} \quad m = \frac{2\nu}{1 + \sin \frac{\theta}{2}} \quad (11)$$

For the plane $\theta = 0$ it turns out that $n=1$ and $m=2\nu$. Furthermore, by taking $\nu = \frac{1}{3}$ the $\mathcal{PCF}=3$. Similar results are obtained by applying other yield criteria. In the case of plane stress $n=1$ and $m=0$, which gives the estimate; $\mathcal{PCF}=1$. For more details see [9].

Therefore, the normal stress σ_{xx} on the $\theta = 0$ plane in plane strain can be as high as three times the yield stress. During plastic deformation the crack tip is blunted. Since a stress perpendicular to a free surface cannot exist, it follows that σ_{xx} must tend to zero at the crack tip. In that case $\sigma_2=0$, i.e. there is a state of plane stress. Consequently, the PCF must drop to 1 and the stress at the crack tip does not exceed the yield stress. In the plane strain case the stress rises quickly from σ_{yield} at the very crack tip to $3\sigma_{yield}$ at a short distance from the crack. This is confirmed by finite element calculations [9]. Again, we note the qualitative agreement with Hill's result, and with somewhat ad-hoc justification, we shall adopt it to provide the stress field for our model problem. Figures 3 and 4 illustrate the hydrostatic stress distributions for the plane stress and plane strain models ahead of the crack.

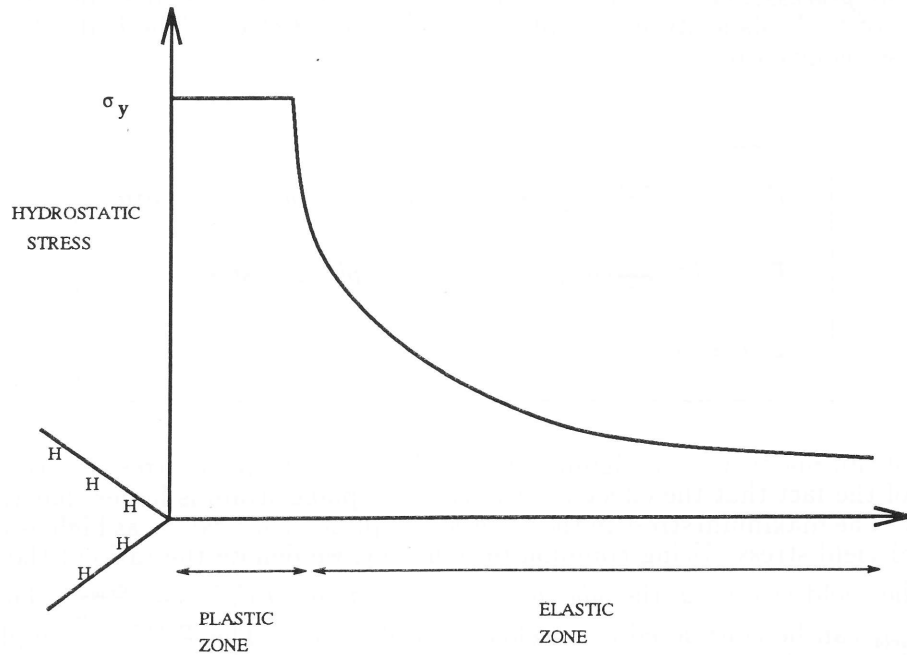


Figure 3: Plane stress distribution of hydrostatic stress ahead of the crack

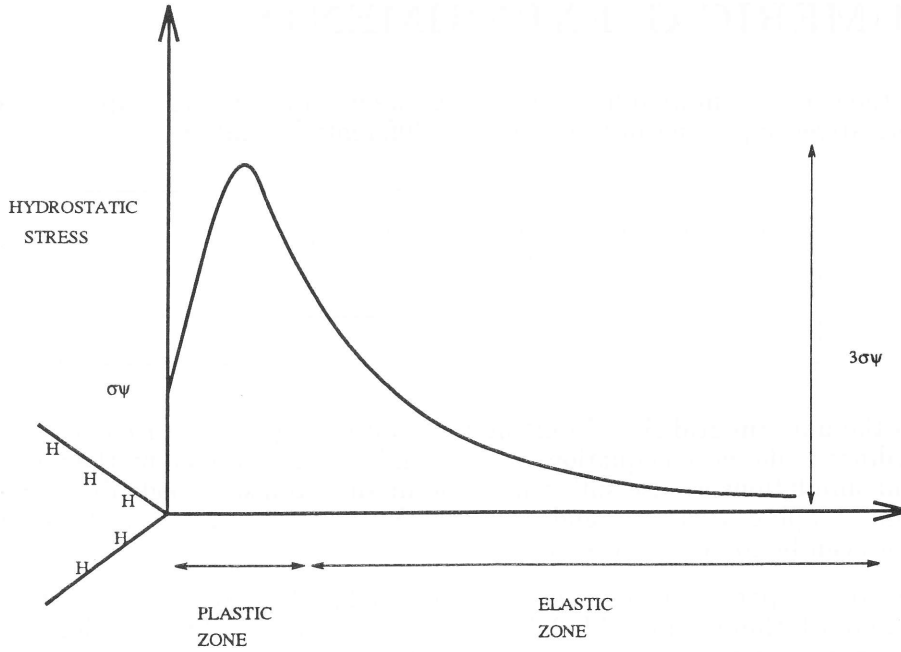


Figure 4: Plane strain distribution of hydrostatic stress ahead of the crack

2.2 Coefficients in the Model

For the plastic zone at $\theta = 0$, the coefficients in the governing diffusion models are

$$\boxed{\begin{aligned} \nabla \mathcal{P} &= -\sigma_{yield} \frac{1}{\rho+x} & \nabla^2 \mathcal{P} &= \sigma_{yield} \frac{1}{(\rho+x)^2} \\ \left| \frac{\text{Reaction}}{\text{Diffusion}} \right| &= \frac{\epsilon \sigma_{yield}}{(\rho+x)^2} & \left| \frac{\text{Convection}}{\text{Diffusion}} \right| &= \frac{\epsilon \sigma_{yield}}{(\rho+x)} & \left| \frac{\text{Reaction}}{\text{Convection}} \right| &= \frac{1}{\rho+x} \end{aligned}} \quad (12)$$

In the elastic zone at $\theta = 0$, the coefficients in the governing diffusion models are

$$\boxed{\begin{aligned} \mathcal{P} &= -\frac{\sigma_1 + \sigma_2 + \sigma_3}{3} = -\frac{2}{3} \frac{K_I(1+\nu)}{\sqrt{2\pi x}} & \nabla \mathcal{P} &= \frac{1}{3} \frac{K_I(1+\nu)}{(2\pi)^{\frac{1}{2}} x^{\frac{3}{2}}} & \nabla^2 \mathcal{P} &= 0 \\ \left| \frac{\text{Reaction}}{\text{Diffusion}} \right| &= 0 & \left| \frac{\text{Convection}}{\text{Diffusion}} \right| &= \frac{\epsilon}{3} \frac{K_I(1+\nu)}{(2\pi)^{\frac{1}{2}} x^{\frac{5}{2}}} & \left| \frac{\text{Reaction}}{\text{Convection}} \right| &= 0 \end{aligned}} \quad (13)$$

3 NUMERICAL EXPERIMENTS

Following the standard finite difference strategy we use a fourth order approximation for the spatial derivatives appearing in the governing differential equation

$$\begin{aligned}\frac{\partial c}{\partial x} &= \frac{-c(x+2h)+8c(x+h)-8c(x-h)+c(x+2h)}{12h} + O(\delta h^4) \\ \frac{\partial^2 c}{\partial x^2} &= \frac{-c(x+2h)+16c(x+h)-30c(x)+16c(x-h)-c(x+2h)}{12h^2} + O(\delta h^4)\end{aligned}\quad (14)$$

where h is the uniform grid size. Inserting these into the governing PDE yields a system of coupled ordinary differential equations whose number is determined by the number of nodes used. In all simulations we use sufficiently fine meshes to insure negligible numerical error. For the time stepping we use a standard Runge-Kutta scheme($\mathcal{O}(\delta t^4)$). A detailed study of the numerics can be found elsewhere[11].

In order to compare with previous experiments [2], we used properties of a commercial 2090 Aluminum-Lithium alloy (AL-2.2Li-2.9Cu-0.12Zr) in the T8 condition. The material was produced in the form of a rolled plate, and its microstructure consists of flat grains with average dimensions $1100\mu m \times 240\mu m \times 11\mu m$. In [2], scanning electron microscopy examinations of the fracture surfaces showed an exclusively intergranular cracking mode. Cracking occurs on parallel but displaced grain boundaries separated by unfractured ligaments. Experimental evidence has revealed the presence of two types of crack arrest markings (CAM). These are macro- and micro-CAM, the latter corresponding to the individual crack advance events, whereas the former correspond to crack arrest sites.

In the numerical experiments it is assumed that the crack front resides at the Macro-CAM sites until the ligaments are fractured by stress environment interactions and the crack propagation process resumes. Thus from experiments, under intergranular HE, the ligament fracture seems to be the slowest step and controls the overall crack velocity. Regarding the individual crack jump velocity, it should be significantly faster. For details of physical experiments refer to [2]. In the numerical experiments the crack plane lies parallel to the flattened grain boundaries. The intergranular grain-boundary hydrogen diffusivity for aluminum-lithium used is $D_{gb} = 2.2 \times 10^{-10} m^2/sec$. In these tests, c_H is the computed hydrogen content, and c_s is the hydrogen content on the surface. The value of ϵ in the governing equation was selected to be $1.88 \times 10^5 m^2/N$, which is a typical value for aluminum alloys.

3.1 Steady State Tests for Al-Li

Table 1 presents the numerically computed hydrogen content and corresponding time to reach steady-state for the two models discussed. The hydrogen concentration is calculated in relation to c_s , which is the concentration at the crack walls. The results show that under plane stress conditions there is no difference between the DCR and DC models. It is also interesting to note that in the DCR model, the maximum hydrogen concentration, even at steady-state, is only 1.8 times that existing at the crack surface (c_s). However, under plane strain conditions, it is evident that high hydrogen concentrations are predicted by the DCR model. The results presented are in line with the notion that ligament fracture is the rate limiting step in the overall fracture process.

Table 1: Numerically computed hydrogen content in the plastic zone for various models.

Time to Steady State(sec)	Average c_H/c_s in P. Z.	Max c_H/c_s in P. Z.	Problem type
640	4.1	8.1	DCR Plane Strain
29300	0.95	1.0	DCR Plane Stress
370	1.4	1.8	DC Plane Strain
29300	0.95	1.0	DC Plane Stress

Figures 5 and 6 show the concentration profiles in front of the crack tip predicted by the DC and DCR models, respectively, under plane strain conditions. It is important to note that with the DCR model it takes approximately 1.4 (Figure 6) seconds to achieve an average hydrogen concentration of $0.95 c_s$ in the plastic zone for Al-Li. In other words, the effect of the reaction term is *immediate*. Note that the final steady state value is independent of the diffusivity since that parameter divides out of the steady state equation. The diffusivity simply controls the time to steady state not the final value.

It is reasonable to believe that after a microcrack has initiated at the plastic/elastic interface, the bonds in the zone between the microcrack and macrocrack have to be sufficiently

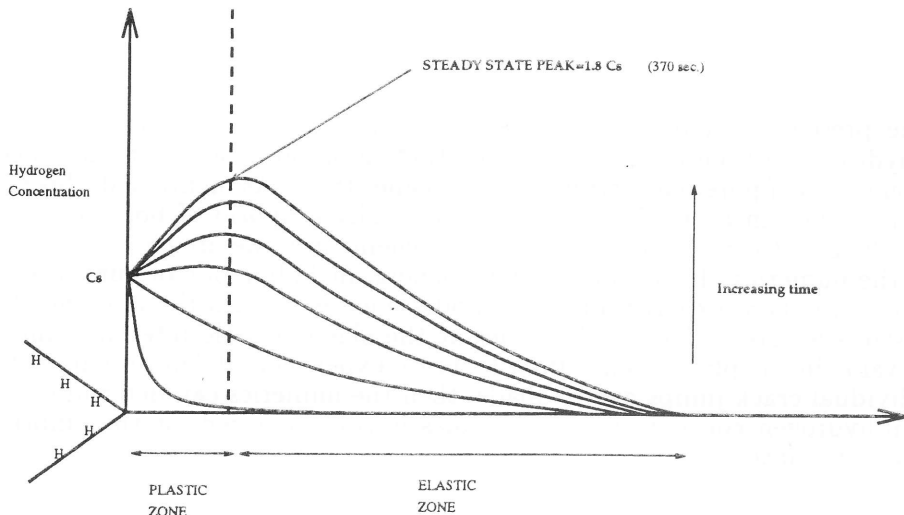


Figure 5: Time transient evolution and steady state profiles of the Diffusion-Convection (DC) solution for the plane strain regime in front of a crack.

weakened for the microcrack to extend backwards to join the macrocrack. This occurs by sufficient hydrogen buildup, which takes an order of magnitude more time. Furthermore, it is then justified to believe that when the average concentration in the plastic zone exceeds some value (depending on the material and some appropriate stress threshold [3] then the microcrack can join the macrocrack by propagating backwards through the sufficiently weakened material. If the initiation is in the vicinity of the original crack, then this microcrack will grow until it rejoins the macrocrack, leading to the appearance of macrocrack "growth" or "propagation".

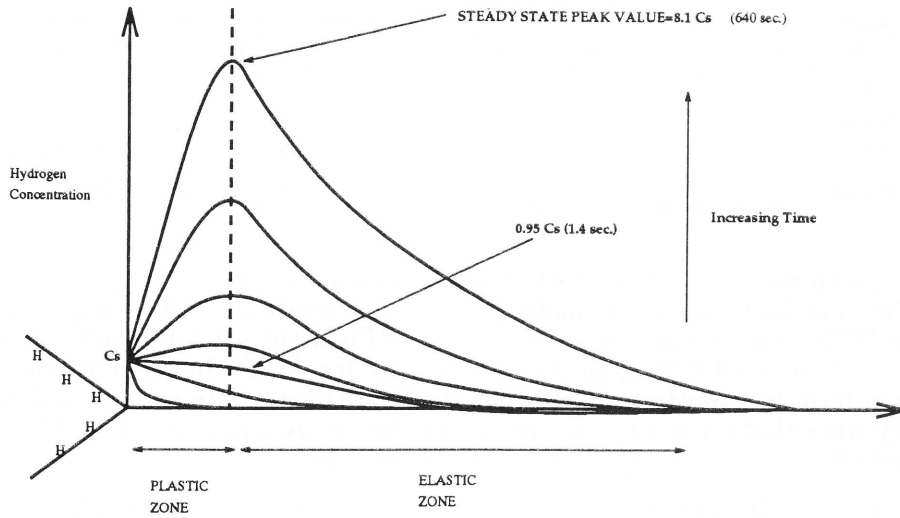


Figure 6: Time transient evolution and steady state profiles of the Diffusion-Convection-Reaction (DCR) solution for the plane strain regime in front of a crack.

From the present simulations it is concluded that the DCR model allows significant buildup of hydrogen in front of the crack. Note that these values are extreme, since the data is based upon states of pure plane strain or pure plane stress. As mentioned, this is rare since cracks typically exist in an environment that is usually a hybrid of both plane strain and plane stress [9]. Due to the high accuracy of the scheme used we are confident that no error stems from the numerics. In several previous papers, including one of ours, the DC model has been used. In these experiments, this model underestimates the amount of hydrogen due to the stress-assisted effect by 4.5 times at the elastic-plastic interface, and 2.9 times the average value in the plastic zone. If an accurate experimental determination of the time between individual crack jumps can be made, then the numerics can determine the average or maximum hydrogen concentration in the plastic zone required for the embrittlement and cracking of the lattice.

4 SUMMARY

The present work has shown that in the presence of inelastic stress fields, and high stress gradients, the neglection of the reaction term in this stress-assisted diffusion model can grossly underestimate the hydrogen diffusion. This is typified by the hydrogen buildup in front of a crack tip, whose corresponding stress field has high gradients and is inelastic. Furthermore, the reaction effect is immediate. Therefore, under these conditions, no time scaling argument can be made to neglect the reaction term.

5 REFERENCES

1. H. P. Van Leeuwen, *A Quantitative Model of Hydrogen Induced Grain Boundary Cracking*, *Corrosion*, 29, 197-204, 1973.
2. T. I. Zohdi and E. I. Meletis, *On the Intergranular Hydrogen Embrittlement Mechanism of Al-Li Alloys*, *Scripta Metall.*, Vol. 26, pp 1615-1620, 1992.
3. P. Doig and T. Jones, *A Model for the Initiation of Hydrogen Embrittlement Cracking at Notches in Gaseous Hydrogen Environments*, *Met. Trans.*, 18A, 1993-1998, 1977.
4. E. C. Aifantis, *A New Interpretation of Diffusion in Regions with High Diffusivity Paths: A Continuum Approach*, *Acta Metall.* 27, 683-691, 1979.
5. E. C. Aifantis, *Some Remarks Concerning the Solid-State Diffusivity Tensor*, *Proceedings of the Sixth Canadian Congress of Applied Mechanics*, 575-958, 1977.
6. D. J. Unger and E. C. Aifantis, *Solutions of Some Diffusion Equations Related to Stress Corrosion Cracking*, *Proceedings Of Conference On Environmental Degradation Of Engineering Materials*, p. 131, VPI Press, Blacksburg, Virginia, 1977.
7. D. J. Unger and E. C. Aifantis, *On the Theory of Stress-Assisted Diffusion, II*, *Acta Mechanica* 47, 117-151, 1983.
8. R. Hill, *The Mathematical Theory of Plasticity*, Clarendon Press, 1950.
9. D. Broek, *Elementary Engineering Fracture Mechanics*, 4th edition, Kluwer Academic Press, 1991.
10. A. U. De Koning, *Results of Calculations with TRIM 6 and TRIAX 6 Elastic-Plastic Elements*, Nat. Aerospace Inst. Amsterdam Rept., Mp 73010, 1973.
11. T. I. Zohdi and E. I. Meletis, *Some Comments on the Numerical Solution to a Stress-Assisted Diffusion Model*, Under Review in *Communications in Numerical Methods in Engineering*, November 1996.